第 34 卷第 6 期
2018 年 6 月

无 机 化 学 学 报
CHINESE JOURNAL OF INORGANIC CHEMISTRY

Vol.34 No.6
1149-1158

# 一维 CdTe@C@$TiO_2$-Au 异质结纳米线的制备及其光催化性能

陈素清　梁华定　金燕仙　沈　茂*
(台州学院医药化工学院,台州　318000)

**摘要**：先利用一步水热法制备了具有核壳结构的 CdTe@C 纳米线,然后以钛酸异丙酯(TIP)作为钛源对 CdTe@C 纳米线进行二氧化钛包覆，最后通过原位还原 $HAuCl_4$ 的方法将 Au 纳米粒子组装到 CdTe@C@$TiO_2$ 表面形成 CdTe@C@$TiO_2$-Au 一维异质结纳米复合材料。用扫描电镜(SEM),X 射线能谱(EDX),透射电镜(TEM),X 射线衍射(XRD),X 射线光电子能谱(XPS)和紫外-可见漫反射光谱(UV-Vis DRS)等对材料进行表征。探究了 CdTe@C@$TiO_2$-Au 催化剂在模拟可见光下降解罗丹明 B(RhB)的光催化性能。实验结果表明：不同催化剂对 RhB 的光降解率不一样，其效果依次为 CdTe@C@$TiO_2$-Au>CdTe@C@$TiO_2$>pure $TiO_2$，其中 CdTe@C@$TiO_2$-Au 能在 270 min 的模拟太阳光下对 RhB 的光降解率达 95.3%,这主要得益于 CdTe、碳层、$TiO_2$ 和具有表面等离子效应的纳米 Au 的共同作用。

**关键词**：纳米线；贵金属；核壳结构；光降解
**中图分类号**：TB34　　**文献标识码**：A　　**文章编号**：1001-4861(2018)06-1149-10
**DOI**:10.11862/CJIC.2018.140

## Fabrication and Photocatalytic Performance of One-Dimensional Structured CdTe@C@$TiO_2$-Au Heteronanowires

CHEN Su-Qing　LIANG Hua-Ding　JIN Yan-Xian　SHEN Mao*
(*College of Pharmaceutical and Chemical Engineering, Taizhou University, Taizhou, Zhejiang* 318000, *China*)

**Abstract:** A novel one-dimensional structured (1D) $TiO_2$-coated CdTe@C nanowires support for Au nanoparticles (CdTe@C@$TiO_2$-Au) is synthesized for photocatalysis application. The structure and properties of the prepared photocatalysts are investigated by X-ray powder diffraction (XRD), scanning transmission electron microscopy (SEM), transmission electron microscopy (TEM), X-ray photoelectron spectra (XPS), and UV-Vis instruments (DRS). As an example of applications, the photodegradation of rhodamine B (RhB) is investigated under the simulated sunlight irradiation. It is found that the photocatalytic activities of these catalysts are 1D CdTe@C@$TiO_2$-Au heteronanowires>CdTe@C@$TiO_2$ nanowires>pure $TiO_2$. Moreover, the degradation rates can reach 95.3% for CdTe @C@$TiO_2$-Au with 270 min of irradiation time. This outcome is attributed to the localized surface plasmon resonance (LSPR) of Au nanoparticles largely enhanced visible light absorption, the efficient photogenerated electron separation of the prepared catalyst and CdTe@C nanowires photosensitized $TiO_2$ structures.

**Keywords:** nanowires; noble metal; core-shell; photodegradation

收稿日期:2017-12-26。收修改稿日期:2018-04-16。
国家自然科学基金项目(No.21403150),浙江省教育厅自然科学基金项目(No.Y201224099)和浙江省教育厅一般科研项目(No.Y201636639)资助。
*通信联系人。E-mail:shenmao19820808@163.com

## 0 Introduction

In the past two decades, titanium dioxide ($TiO_2$), as an excellent photocatalyst, has been widely studied in various degradation of environmental pollutants. In spite of its high chemical stability, nontoxicity, low cost, and excellent degradation for organic pollutants, it can't effectively utilize visible light in solar energy due to its large band gap (about 3.2 eV). In order to improve utilization rate of visible-light region and the photocatalytic activity of $TiO_2$, many studies have been performed by photosensitizing $TiO_2$ structures with narrow band gap semiconductors such as CdS, CdSe, CdTe et al.[1-5], carbonaceous materials and deposition of noble metals on the surface of $TiO_2$[6-9]. Among various small band gap semiconductors, CdTe ($E_g$=1.5 eV) is considered to be one of the most likely candidates due to its unique electrochemical properties, and has been used in photo-electronchemical process. For example, Li has reported an efficient way to synthesize the CdTe quantum dots (QDs)-doped $TiO_2$ photocatalysts, which exhibits much higher photocatalytic activities than both controlled $TiO_2$ (without doped CdTe QDs) and P25 ($TiO_2$, Degussa)[4]. Liu has reported an efficient way to synthesize the samenvatting reduced graphene oxide and CdTe nanoparticles co-decorated $TiO_2$ nanotube array as a visible light photocatalyst[10]. On the other hand, the noble metal nanoparticle based on photocatalysts can assist the electrons transfer and the efficient harvesting of visible-light[11-12]. In addition, carbonaceous materials, due to their wide visible light absorption and high adsorption of organic pollutants, which facilitate the interface reaction of photocatalysis, have received particular attention[13-14]. But so far, there are limited reports about using CdTe-Carbon-$TiO_2$-Noble metal system as photocatalyst for degradation of dye. In particular, the CdTe nanowires based on plasmonic photocatalysts has not been reported. Therefore, it is critical to develop a novel one-dimensional structured CdTe@C@$TiO_2$-Au heteronanowires for enhanced photocatalytic properties.

In the present study, efficient strategy for the synthesis of 1D CdTe@C@$TiO_2$-Au heteronanowires for enhanced photocatalytic properties by a facile, efficient and controllable approach is proposed. The preparation procedure is shown in Scheme 1. First, CdTe@C nanowires are synthesized by one-step hydrothermal process. Next, the CdTe@C@$TiO_2$ nanowires are prepared by the solvothermal method using TIP as titanium source. Finally, Au nanoparticles, which are dispersed on the CdTe@C@$TiO_2$ nanowires by in situ reduction of $HAuCl_4$. Then, this prepared photocatalyst is studied for the photocatalytic degradation rate of RhB under the simulated sunlight irradiation.

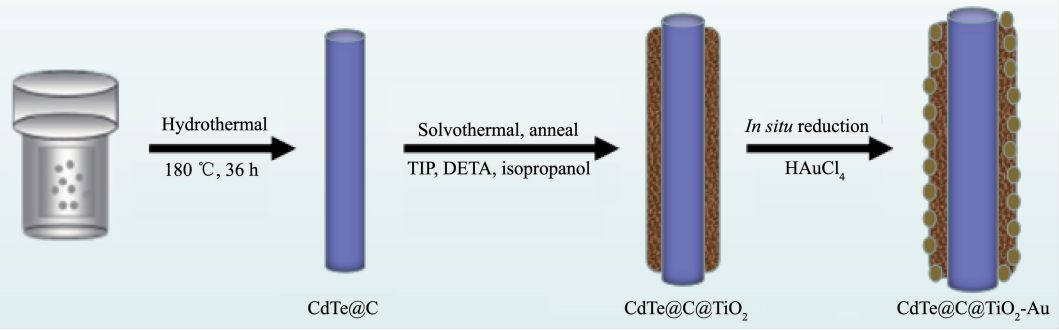


Scheme 1 Preparation procedure of the CdTe@C@$TiO_2$-Au core-shell heteronanowires

## 1 Experimental

### 1.1 Reagents and materials

Ascorbic acid ($C_6H_8O_6$), cetyltrimethy-lammoniumbromide (CTAB), sodium tellurite ($Na_2TeO_3$), cadmiumchloride ($CdCl_2 \cdot 2.5H_2O$), anhydrous ethanol, and isopropanol were purchased from Guangfu Fine Chemical Research Institute (Tianjin, China); Titanium isopropoxide (TIP, 97%), diethylenetriamine (DETA) and chloroauric acid ($HAuCl_4 \cdot 4H_2O$) were purchased from Sigma-Aldrich.

### 1.2 Instruments

TEM images were obtained on a JEM-2100 TEM (JEOL Ltd., Tokyo, Japan, 200 kV). XRD analysis was performed using a Dmax-2500 (Rigaku Corporation, Tokyo, Japan, Cu $K\alpha$, $\lambda$=0.154 06 nm, $U$=40 kV, $I$=40 mA), analyzed samples were scanned from 10° to 80° at a scanning rate of 10 ℃·$min^{-1}$. SEM was carried out on a Philips XL30 microscope (Philips, Amsterdam, Netherlands) coupled to an EDAX DX4i analyzer for energy-dispersive X-ray analysis at 20 kV. XPS analysis was recorded by Thermo ESCALAB 250XI X-ray photoelectron spectrometer (Thermo Fisher Scientific Inc., Waltham, MA, USA) with a monochromatized Al $K\alpha$ X-ray source (1 486.6 eV) at a constant dwell time of 50 ms and a pass-energy of 50 eV. The UV-Vis absor-ption spectra of all the samples were obtained using a U-4100 spectro-photometer (Shimadzu, Tokyo, Japan).

### 1.3 Synthesis and preparation

#### 1.3.1 Synthesis of CdTe@C core-shell nanowires

The core-shell CdTe@C nanowires were synthesised according to previously reported[15]. 1.0 g ascorbic acid ($C_6H_8O_6$) and 0.3 g CTAB were dissolved in 70 mL of deionized water, 0.5 g $Na_2TeO_3$ and 0.52 g $CdCl_2 \cdot 2.5H_2O$ were added to the above solution in order; a white $TeO_2$ was precipitated immediately upon the addition of the $Na_2TeO_3$ then, the above solution was transferred into a 100 mL Teflon-lined stainless steel autoclave. Finally, the reaction was maintained at 180 ℃ for 36 h in a preheated electric oven. The black products were collected and washed repeatedly with deionized water and ethanol, then dried at 60 ℃ for 12 h.

#### 1.3.2 Synthesis of CdTe@C@$TiO_2$ one-dimensional nanowires

First, 0.1 g CdTe@C nanowires were dispersed into 70 mL isopropanol, and then 0.03 mL DETA and 1.5 mL TIP were added into the obtained solution. The above solution was subsequently transferred into a 100 mL Teflon-lined stainless steel autoclave and kept in an electric oven at 200 ℃ for 24 h. When the reaction kettle was left to cool down to room temperature, the black products were collected after washing, centrifugation, and drying. Finally, the prepared CdTe@C@$TiO_2$ was treated at 450 ℃ in $N_2$ for 2 h with a heating rate of 1 ℃·$min^{-1}$ to obtain highly crystalline phase.

#### 1.3.3 Synthesis of CdTe@C@$TiO_2$-Au one-dimensional heteronanowires

0.1 g CdTe@C@$TiO_2$ heteronanowires and 1 mL (0.01 g·$mL^{-1}$) $HAuCl_4$ were dispersed into 100 mL deionized water, the solution was heated and kept boiling under vigorous stirring for 10 minutes. Then 5 mL (0.01 g·$mL^{-1}$) aqueous solution of sodium citrate were injected into the above solution, the reaction proc-eeded for 15 min. Finally, the CdTe@C@$TiO_2$-Au heteronanowires were collected after washing, centrifugation and drying.

Pure $TiO_2$ nanoparticles were obtained using a similar procedure to the above without CdTe@C nanowires.

### 1.4 Photocatalytic activity of the CdTe@C@$TiO_2$-Au heteronanowires

Photocatalytic activity of the CdTe@C@$TiO_2$-Au heteronanowires was evaluated by the degradation of RhB under the simulated sunlight irradiation by a 500 W Xe arc lamp. The experiments were as follows: 0.03 g the prepared photocatalyst was dispersed in a 150 mL (25 mg·$L^{-1}$) RhB aqueous solution. After reaching the adsorption-desorption equilibrium among the photocatalyst, RhB, and water, the reaction began under light irradiation, the RhB solution was filtrated to measure for every 30 min. The absorption of RhB was determined by an UV-Visible spectrophotometer (UV-4510, Shimadzu, Japan). Total organic carbon (TOC) of the RhB solution was measured with a Shimadzu TOC-VCPH analyzer.

## 2 Results and discussion

### 2.1 Characterization of CdTe@C@$TiO_2$-Au heteronanowires

XRD patterns of the synthesized CdTe@C@$TiO_2$-Au, CdTe@C, CdTe@C@$TiO_2$ nanowires are shown in Fig.1. As shown in Fig.1, the five diffraction peaks of CdTe are clearly seen at 23.9°, 39.5°, 46.5°, 57.1° and 62.6° of all the samples, which are indexed to the

(111), (220), (311), (331) and (400) planes of the zinc-blende CdTe (PDF No.15-0770). As shown in Fig.1b, after deposition of $TiO_2$ nanoparticles onto the CdTe@C nanowires, the additional diffraction peaks at $2\theta$= 25.5°, 38.1°, 48.2°, 54.3°, and 55.0° assigned to the (101), (004), (200), (211) and (204) planes (PDF No. 89-4921) are obviously observed[16]. In comparison with the CdTe@C@$TiO_2$ nanowires, after grafting of Au nanoparticles on the surface, the typical diffraction peaks of Au nanoparticles can be detected (Fig.1c), which are in agreement with the standard values of gold (PDF No.04-0784).

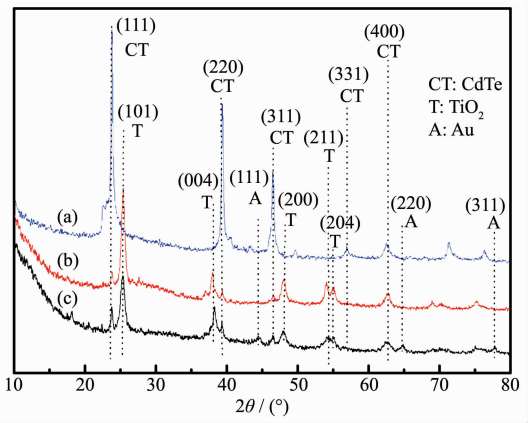


Fig.1 XRD patterns of (a) CdTe@C, (b) CdTe@C@$TiO_2$ and (c) CdTe@C@$TiO_2$-Au

The morphology of synthesized CdTe@C, CdTe@C@$TiO_2$, and CdTe@C@$TiO_2$-Au nanowires are characterized by SEM and TEM. As can be seen in Fig.2(a, d), the as-prepared CdTe@C nanowires exhibit the average diameter of one-dimensional morphology is about 50 nm and the lengths is longer than 1 μm, which is consistent with the previous reports [15,17]. Moreover, it is obvious that the carbon shell of CdTe@C nanowires is about 10 nm. As can be seen in Fig.2 (b,e), after deposition of $TiO_2$ nanoparticles onto the CdTe@C nanowires, the average diameter of the CdTe@C@$TiO_2$ is about 150 nm. It is obvious that the uniformly $TiO_2$ nanoparticles are densely coated on the surface of CdTe@C nanowires forming the one-dimensional CdTe@C@$TiO_2$ nanowires. As can be seen in Fig.2(c,f), after loading Au nanoparticles on the surface of CdTe@C@$TiO_2$ nanowires, the average diameter of Au nanoparticles (10 nm) (inset of Fig.2f) is successfully coated on the surface of CdTe@C@$TiO_2$ nanowires.

In order to analyze the chemical composition of the synthesized CdTe@C, CdTe@C@$TiO_2$, and CdTe@C@$TiO_2$-Au nanowires, the EDX spectrum was obtained

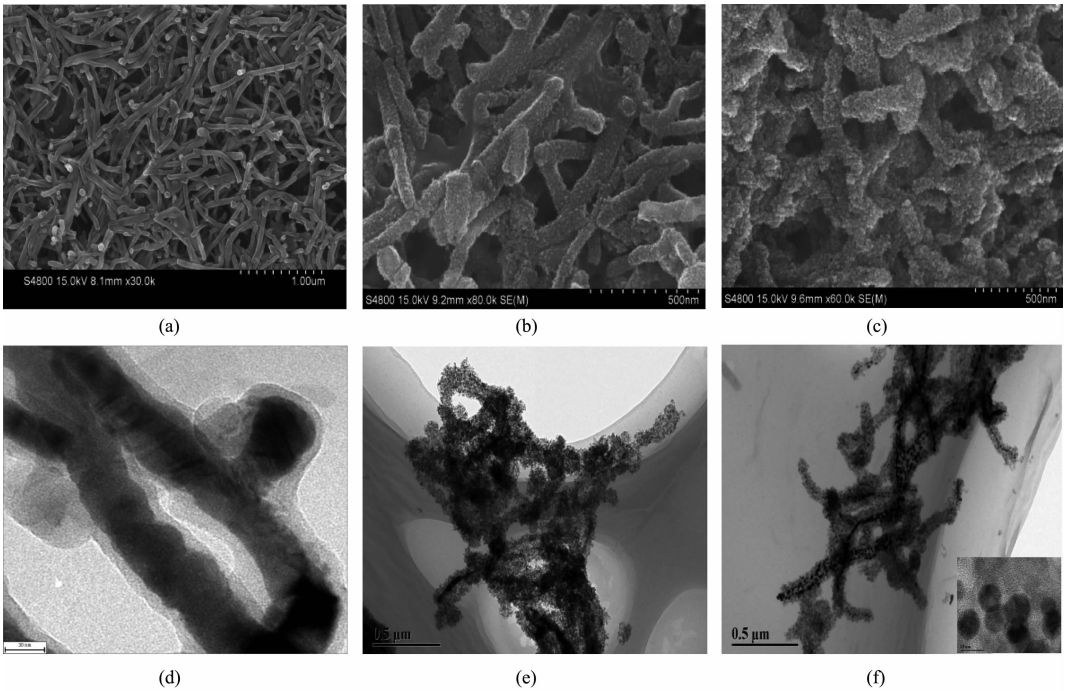


Fig.2 SEM and TEM images of (a, d) CdTe@C nanowires, (b, e) CdTe@C@$TiO_2$ nanowires and (c, f) CdTe@C@$TiO_2$-Au nanowires

for the above one-dimensional structure. As can be seen in Fig.3a, the spectrum reveals the presence of Cd, Te, and C peaks in the CdTe@C nanowires structure. After deposition of $TiO_2$ onto the CdTe@C nanowires, the presence of Cd, Te, C, Ti and O peaks in the CdTe@C@$TiO_2$ nanowires structure is confirmed (Fig.3b). After loading Au nanoparticles on the surface of CdTe@C@$TiO_2$ nanowires, it is clearly seen that the additional Au element appears (Fig.3c), which indicates that the Au nanoparticles have been loaded successfully. Furthermore, the spatial distribution of each element in these structures is investigated by the electron mapping image analysis as shown in Fig.4(a~f).

XPS spectra are collected to determine the chemical composition and identify the chemical states of the as-prepared CdTe@C@$TiO_2$-Au samples in Fig. 5. Fig.5a shows the fully XPS spectra, it reveals the presence of Cd, Te, C, Ti, O and Au elements in the CdTe@C@$TiO_2$-Au, which is consistent with the analysis of EDX and elemental mappings. As shown in Fig.5b, the Cd3*d* spectrum displays two peaks at 405.3 and 412.0 eV, which are attributed to the Cd in the CdTe[18]. The Te3*d* spectrum appears at 571.8 and 582.2 eV, which are corresponded to the Cd-Te bonding states in Fig.5c[18]. In the Au4*f* spectrum (Fig.5d), the binding energies of the peaks at 87.7 and 84.1 eV are Au4$f^5$ and Au4$f^7$ [19], respectively. Fig5(e,f) displays the C1*s* and O1*s* spectra, respectively. The peaks with binding energy of 284.8 and 531.7 eV are correspond to the C-C skeleton and an -OH group[18,20]. Fig.5g displays the Ti spectrum, the two peaks at 464.1 and 458.4 eV can be attributed to the Ti2$p_{1/2}$ and Ti2$p_{3/2}$,

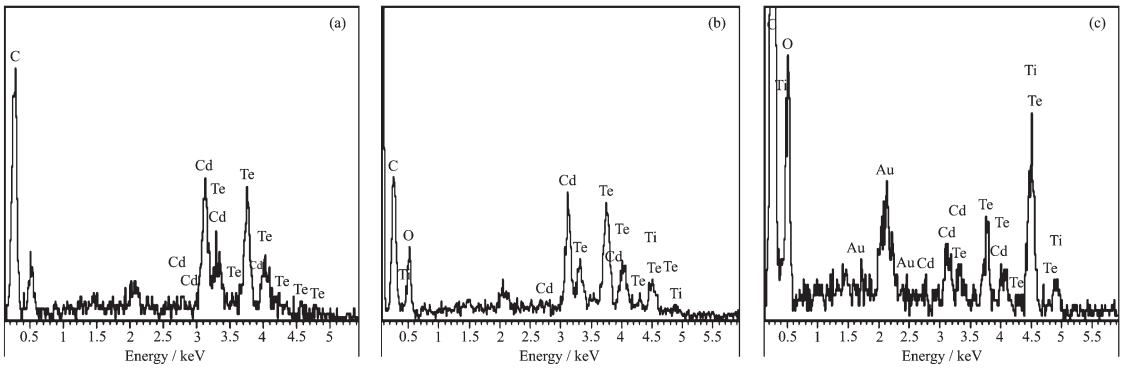


Fig.3　EDX spectra of (a) CdTe@C nanowires, (b) CdTe@C@$TiO_2$ nanowires and (c) CdTe@C@$TiO_2$-Au nanowires

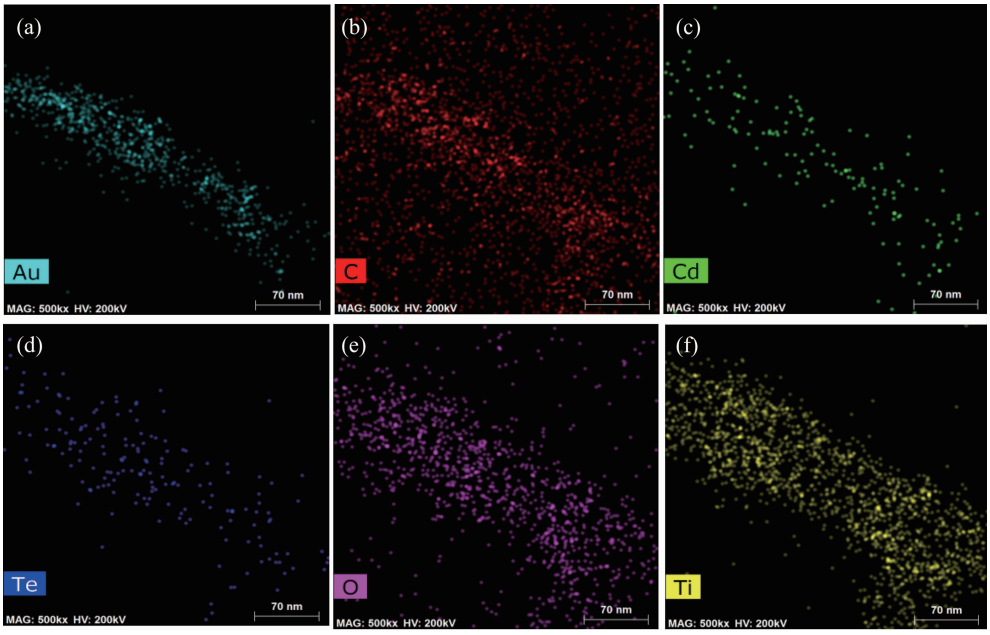


Fig.4　Elemental mappings of Au, C, Cd, Te, O and Ti in the CdTe@C@$TiO_2$-Au nanowires

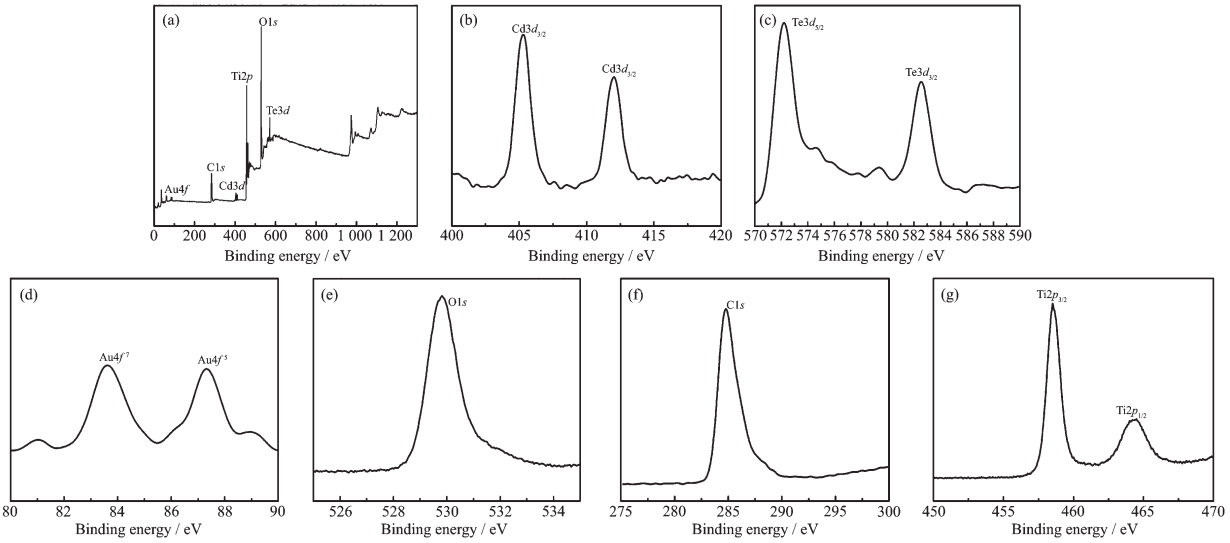


(a) wide scan; (b) Cd3*d*; (c) Te3*d*; (d) Au4*f*; (e) O1*s*; (f) C1*s*; (g) Ti2*p*

Fig.5 XPS spectra of CdTe@C@$TiO_2$-Au nanowires

respectively, which are assigned to the $Ti^{4+}$ oxidation state according to reported XPS data[21].

To investigate the optical property of the as-prepared CdTe@C nanowires, the samples are characterized by absorption spectra. The spectrum ((Fig.6a) reveals that the CdTe@C nanowires have low absorption in the NIR (near infrared reflection) region, whereas the absorption is high in the UV-Vis regions. Based on their absorption spectra, the variation in the absorption coefficient as a function of photon energy for allowed direct transitions is given by:

$$\alpha h\nu = A(h\nu - E_g)^{1/2} \quad (\mathbf{1})$$

where $\alpha$ is the absorption coefficient, $A$ is a constant, $h$ is Planck′s constant, $\nu$ is the frequency, and $E_g$ is the band gap energy. The $E_g$ value is obtained by extrapolating the linear part to intercept with the energy axis (Fig.6b) and is found to be 2.25 eV.

Furthermore, the optical properties of the as-prepared (a) pure $TiO_2$ nanoparticles, (b) CdTe@C@$TiO_2$ nanowires and (c) CdTe@C@$TiO_2$-Au nanowires are investigated by UV-Vis diffuse reflectance spectra (Fig.7). As shown in Fig.7a, the absorption peak of the pure $TiO_2$ nanoparticles is around 315 nm, and there is almost no absorption of visible light. In contrast to the pure $TiO_2$, after coating a layer of porous $TiO_2$ shell on the surface of CdTe@C, the strong absorption in visible light region was appeared due to the synergistic effect of CdTe@C@$TiO_2$ nanowires (Fig.7b). As shown in Fig.7c, it is evident that the absorption in visible light region is further improved due to the surface plasmon of Au nanoparticles.

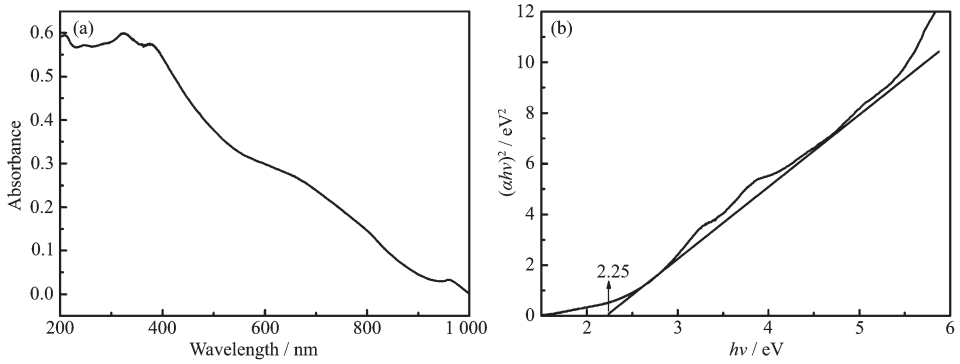


Fig.6 (a) Optical absorption spectrum of CdTe@C nanowires and (b) $(\alpha h\nu)^2$ versus $h\nu$ plot

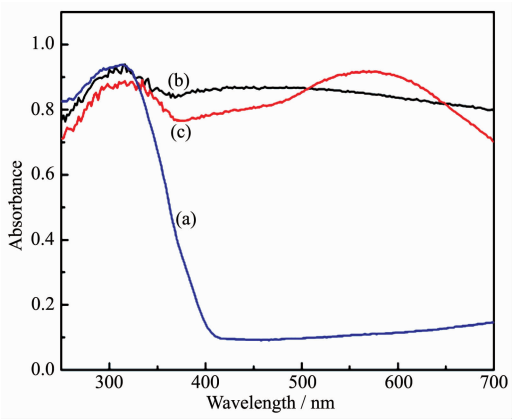


Fig.7　UV-Vis spectroscopy of (a) pure $TiO_2$ nanoparticles, (b) CdTe@C@$TiO_2$ nanowires and (c) CdTe@C@$TiO_2$-Au nanowires

## 2.2　Photocatalytic activities of the CdTe@C@$TiO_2$-Au nanowires

The photocatalytic activities of CdTe@C@$TiO_2$-Au nanowires are evaluated through the RhB degradation under the simulated sunlight irradiation. Fig.8(a~c) display the absorption spectra of RhB solutions by different photocatalyst, respectively. It is clearly seen that the absorption peak at 552.5 nm diminishes gradually as time go on for all the samples. Furthermore, it is also clearly seen that the degradation activities of CdTe@C@$TiO_2$-Au nanowires are higher than CdTe@C@$TiO_2$ nanowires and pure $TiO_2$.

In addition, as shown in Fig.9a, it can be clearly observed that the degradation rates reach 95.3% for CdTe@C@$TiO_2$-Au nanowires, 68.3% for CdTe@C@$TiO_2$, and 43.1% for pure after 270 min of simulated sunlight illumination, where $C$ is the initial concentration before the dark reaction and $C_t$ is a concentration of reaction time. The outstanding photocatalytic degradation activities of the CdTe@C@$TiO_2$-Au nanowires are mainly due to the following advantages: (1) the LSPR of Au metals enhances plasmonic absorption in visible light region; (2) Au nanoparticles effectively improve the separation of photogenerated $e^-/h^+$ pairs in the $TiO_2$ shell; (3) The CdTe@C nanowires offere more pronounced photon absorption due to the photosensi-

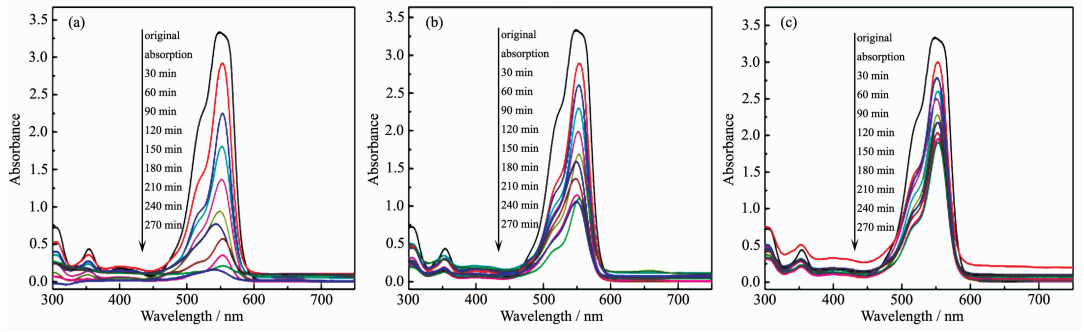


Fig.8　Absorption spectra of photocatalytic degradation of RhB solution under different photocatalysts of (a) CdTe@C@$TiO_2$-Au nanowires, (b) CdTe@C@$TiO_2$ nanowires and (c) pure $TiO_2$

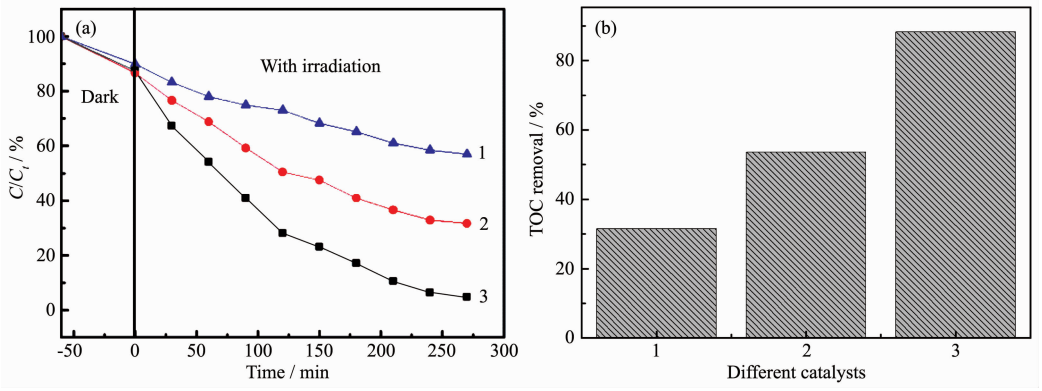


(1) Pure $TiO_2$, (2) CdTe@C@$TiO_2$ and (3) CdTe@C@$TiO_2$-Au nanowires

Fig.9　(a) Degradation rate of RhB solution under different photocatalysts; (b) TOC removal rates under different photocatalysts after 270 min simulated sunlight illumination

tization of $TiO_2$ structures[10]. Meanwhile, the TOC removal in the catalytic process is also measured. As shown in Fig.9b, CdTe@C@$TiO_2$-Au nanowires exhibit the best catalytic performance for RhB mineralization. The initial TOC value of RhB is 24.29 mg·$L^{-1}$, and the results show that the TOC removal (2.85 mg·$L^{-1}$) rates reach 88.3% for CdTe@C@$TiO_2$-Au nanowires, 53.6% (11.27 mg·$L^{-1}$) for CdTe@C@$TiO_2$, and 31.49% (16.64 mg·$L^{-1}$) for pure $TiO_2$ after 270 min of simulated sunlight illumination. The results of TOC removal are consistent with Fig.9a. However, the TOC measurements show that complete mineralization (conversion of all carbon atoms to CO or $CO_2$) cannot be achieved. This indicates that some small organic compounds (aldehydes, carboxylic acids *etc.*) still remain when the chromophores (aromatic rings) are completely broken.

On the other hand, the kinetics of catalytic degradation of RhB in different samples is used to quantify the catalytic efficiency with the following equation:

$$\ln(C_0/C_t)=kt \quad (2)$$

Where $C_0$ is the initial concentration after the dark reaction, $k$ is a rate constant, $t$ is time, $R^2$ is coefficient of determination.

Linear relationships between $\ln(C_0/C_t)$ and the reaction time are displayed in Fig.10(a~c), which matched well with the first-order reaction kinetics. When the system is performed with the CdTe@C@$TiO_2$-Au nanowires as catalysts, the rate constant $k$ (Fig.10a) is calculated to be 0.010 07 $min^{-1}$, which is higher than CdTe@C@$TiO_2$ nanowires ($k$=0.003 97 $min^{-1}$, in Fig.10b) and pure $TiO_2$ ($k$=0.001 79 $min^{-1}$, in Fig.10c).

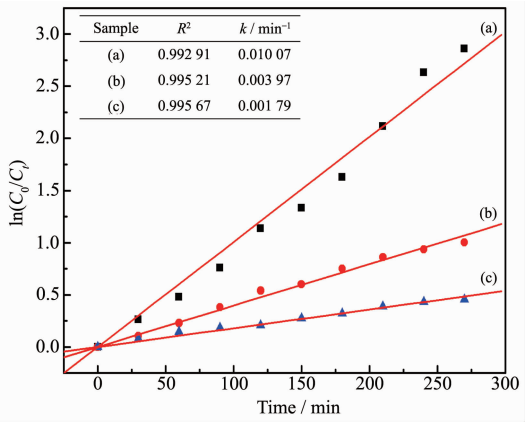


Inset is the parameters of kinetics plots

Fig.10 Kinetics of catalytic degradation of RhB under different photocatalysts of (a) CdTe@C@$TiO_2$-Au nanowires, (b) CdTe@C@$TiO_2$ nanowires and (c) pure $TiO_2$

In order to investigate the stability of CdTe@C@$TiO_2$-Au nanowires in the photocatalytic RhB system, the CdTe@C@$TiO_2$-Au is reused by centrifugalization. As presented in Fig.11, the catalytic activity of CdTe@C@$TiO_2$-Au decreases slightly obviously after recycling for four times. This may be due to the agglomeration and the loss of Au nanoparticles during repeated reuse.

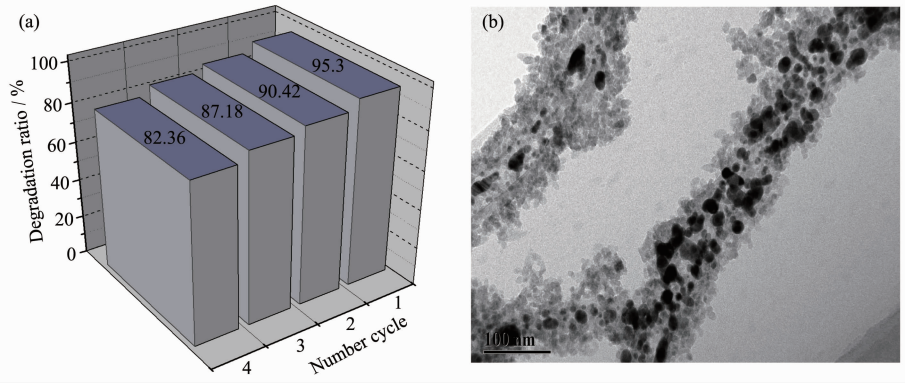


Fig.11 (a) Degradation rate of RhB in 270 min by CdTe@C@$TiO_2$-Au for four cycles; (b) TEM image of CdTe@C@$TiO_2$-Au after four cycles

## 2.3 Photocatalysis mechanism

In general, the band structure of the photocatalyst is responsible for the efficient generation and separation process of the electron-hole pairs. The

band positions of CdTe@C nanowires can be calculated by the following empirical formulas[22]:

$$E_{VB}=X-E^e+0.5E_g \quad (3)$$

$$E_{CB}=E_{VB}-E_g \quad (4)$$

where $E_{VB}$ is the valence band (VB) potentials, $E_{CB}$ is the conduction band (CB) potential, $X$ is the electronegativity of the semiconductor (which is the geometric mean of the electronegativity of the constituent atoms), $E^e$ is the energy of free electrons on the hydrogen scale (~4.5 eV), $X$ is the electronegativity of the semiconductor (5.3 eV for CdTe@C). Therefore, $E_{VB}$ of CdTe@C is 1.93 eV, $E_{CB}$ of CdTe@C is −0.32 eV, $E_{VB}$ of $TiO_2$ is 3.0 eV, $E_{CB}$ of $TiO_2$ is −0.2 eV. In addition, the Au nano-particles decorated on the surface of semiconductor can act as electron trap to promote the separation of photogenerated charge carriers, absorb visible light and generate electrons due to the LSPR effect as well.

Based on the above discussion, we proposed a complete photocatalytic mechanism for the 1D CdTe@C@$TiO_2$-Au nanowires under the simulated sunlight irradiation as illustrated by formulae (**5~11**).

Existing literatures show that CdTe has a high optical absorption capacity for visible light as a narrow band gap energy semiconductor at room temperature[23]. By controlling the morphological parameters of CdTe from quantum dot to nanowires, a wide range of band gap energies in the visible spectrum can be formed[24-25]. In addition, CdTe nanowires with carbon can not only make itself more stable, but also improve the visible light photocatalytic activity[13]. When the CdTe@C@$TiO_2$-Au catalyst was exposed to an Xe lamp, the materials of CdTe nanowires and $TiO_2$ are excited (formula **5**). Then, the photoexcited electron migrates from the conduction band of CdTe ($CB_{CdTe}$) to the conduction band of $TiO_2$ ($CB_{TiO_2}$), leaving the photogenerated holes in the valence band of CdTe ($VB_{CdTe}$), and the photogenerated holes of $TiO_2$ move from the $VB_{TiO_2}$ to the $VB_{CdTe}$, which can hinder the recombination of electron and holes (formula **6**)[18]. In addition, the Au nanoparticles decorated on the surface of 1D CdTe@C@$TiO_2$ can not only act as electron trap to promote the separation of photogenerated charge carriers, but also can absorb visible light and generate electrons due to the surface plasmon resonance effect (formulae **7** and **8**). At last, the photogenerated holes react with $H_2O$ to form ·OH (formula **9**). Meanwhile, the photogenerated electrons react with the $O_2$ on the surface of catalyst or in the solution to form $\cdot O_2^-$ (formula **10**). Finally, the Rhodamine B are degraded by ·OH and $\cdot O_2^-$ radicals (formula **11**). In order to intuitively understand the charge separation and transfer between CdTe@C, $TiO_2$ and Au under the simulated sunlight irradiation, the synergetic mechanism of the electron-hole separation is illustrated in Scheme 2.

$$TiO_2+CdTe+h\nu \rightarrow TiO_2(e^-+h^+)+CdTe(e^-+h^+) \quad (5)$$

$$CdTe(e^-)+TiO_2 \rightarrow TiO_2(e^-)+CdTe \quad (6)$$

$$Au+h\nu \rightarrow Au\ (e^-) \quad (7)$$

$$TiO_2(e^-)+Au \rightarrow TiO_2+Au(e^-) \quad (8)$$

$$CdTe(h^+)+H_2O \rightarrow CdTe+\cdot OH+H^+ \quad (9)$$

$$Au(e^-)+O_2 \rightarrow Au+\cdot O_2^- \quad (10)$$

$$\text{rhodamine B}+\cdot OH+\cdot O_2^- \rightarrow \text{degradation products} \quad (11)$$

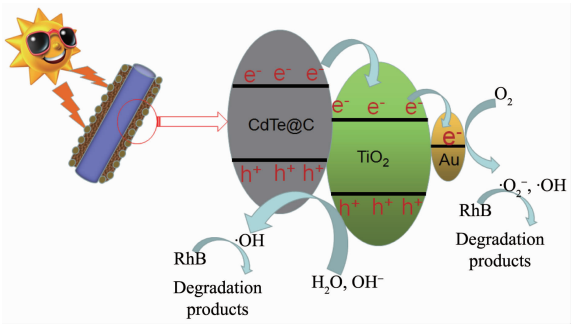


Scheme 2　Mechanism of charge separation and transfer between CdTe@C, $TiO_2$ and Au nanoparticles under the simulated sunlight irradiation

## 3　Conclusions

In conclusion, we have successfully synthesized a novel 1D structured $TiO_2$-coated CdTe@C nanowires support for Au nanoparticles. The characterization results confirm that the 1D morphology of CdTe@C@$TiO_2$-Au nanowires with an average diameter of about 150 nm (the lengths>1 μm) combines the strong light harvesting capability. This ternary design can not only enhance the absorption in visible region, but also promote the photogenerated electron/hole separation.

Consequently, it is found that the resultant 1D CdTe@C@$TiO_2$-Au heteronanowires have much higher photocatalytic effect of RhB than that of CdTe@C@$TiO_2$ nanowires and pure $TiO_2$, and the degradation rates can reach 95.3% for CdTe@C@$TiO_2$-Au with 270 min of irradiation time.

**Acknowledgments:** This study is funded by the National Natural Science Fund (Grant No.21403150), the General research project of Zhejiang Provincial Department of Education (Grant No.Y201636639) and the Scientific Research Fund of Zhejiang Provincial Education Department (Grant No.Y201224099).

## References:

[1] Banerjee S, Mohapatra S K, Das P P, et al. *Chem. Mater.*, **2015**,**20**(21):6784-6791

[2] Kim J C, Choi J, Lee Y B, et al. *Chem. Commun.*, **2006**,**48**(48):5024-5026

[3] Ho W, Yu J C. *J. Mol. Catal. A*: *Chem.*, **2006**,**247**(1):268-274

[4] Li Y S, Jiang F L, Xiao Q, et al. *Appl. Catal., B*, **2010**,**101**(1):118-129

[5] XIANG Yu(向宇), FU Ji-Jiang(付继江), HE Na(赫娜), et al. *Chinese J. Inorg. Chem.*(无机化学学报), **2013**,**29**(6):1215-1221

[6] Li H X, Bian Z F, Zhu J, et al. *J. Am. Chem. Soc.*, **2007**,**129**(15):4538-4539

[7] LIU Li-Fen(柳丽芬), DONG Xiao-Yan(董晓艳), YANG Feng-Lin(杨凤林), et al. *Chinese J. Inorg. Chem.*(无机化学学报), **2008**,**24**(2):211-217

[8] KOU Shu-Fang(寇书芳), FENG Zhen-Yu(封振宇), WANG Chun-Xing(王春省), et al. *Chinese J. Inorg. Chem.*(无机化学学报), **2017**,**33**(8):1390-1396

[9] Wang R H, Wang X W, Xin J H. *ACS Appl. Mater. Interface*, **2014**,**2**(1):82-85

[10]Liu M J, Lei H, Liu X N, et al. *J. Mater. Sci.*, **2014**,**49**(5):2263-2269

[11]Zhang N, Liu S Q, Fu X Z, et al. *J. Phys. Chem. C*, **2011**, **115**(18):9136-9145

[12]Chen S F, Li J P, Qian K. *Nano Res.*, **2010**,**3**(4):244-255

[13]Zhuang J D, Tian Q F, Zhou H, et al. *J. Mater. Chem.*, **2012**,**22**(14):7036-7042

[14]Wang D H, Jia L, Wu X L, et al. *Nanoscale*, **2012**,**4**(2):576-584

[15]Hadia N M, Awad M A, Mohamed S H. *Appl. Phys. A*, **2016**, **122**(10):889-893

[16]LI Liang(李亮), LIU Li-Fen(柳丽芬), YANG Feng-Lin(杨凤林). *Chinese J. Inorg. Chem.*(无机化学学报), **2017**,**33**(4):637-643

[17]Yong S M, Muralidharan P, Jo S H. *Mater. Lett.*, **2014**,**64**(14):1551-1554

[18]Zhu W F, Pan S G, Wang W W, et al. *New J. Chem.*, **2013**, **37**(9):2751-2757

[19]Shen M, Chen S Q, Jia W P, et al. *Gold Bull.*, **2016**,**9**(3/4):103-109

[20]Zheng Y Z, Xu Y Y, Fang H B, et al. *RSC Adv.*, **2015**,**5**(126):103790-103796

[21]Dong Q S, Yu H C, Jiao Z B, et al. *RSC Adv.*, **2014**,**4**(103):59114-59117

[22]Guan M L, Ma D K, Hu S W, et al. *Inorg. Chem.*, **2011**,**50**(3):800-805

[23]Zhang W G, Liu J, Guo Z Y, et al. *J. Mater. Sci.*: *Mater. Electron.*, **2017**,**28**(13):9505-9513

[24]Fang J, Xu L, Zhang Z Y, et al. *ACS Appl. Mater. Interface*, **2013**,**5**(16):8088-8092

[25]Liang X R, Tan S S, Tang Z Y. *Langmuir*, **2004**,**20**(4):1016-1020